6th International Symposium on Space Sailing (ISSS 2023), New York, USA, 5-9 June 2023

Optimal deep-space heliocentric transfers with an electric sail and an electric thruster

Lorenzo NICCOLAI[a,*]

[a]*Department of Civil and Industrial Engineering, University of Pisa, Pisa, Italy*

Abstract

An electric solar wind sail is a propellantless propulsive system that generates thrust by exploiting the interaction of solar wind ions and one or more charged tethers. Assuming a realistic scenario in which the sail is composed by a limited number of tethers, the generated propulsive acceleration vector has a small magnitude, and it is constrained to lie in a cone centered on the outward radial direction with half-angle equal to about 20 degrees. In order to overcome this issue, a possible strategy consists in combining the sail with an electric thruster, which should provide a small thrust steerable around the circumferential direction. The effectiveness of such a combination is thoroughly analyzed in this work. Transfer trajectories are obtained as outputs of a multi-objective optimization, in which a suitable linear function of the flight time and the propellant consumption is minimized, considering different relative weights of the two competing requirements. Two exemplary case studies, consisting of Earth-Mars and Earth-Venus circle-to-circle transfers, are presented to show the effectiveness of the proposed strategy.

Keywords: electric solar wind sail, electric propulsion, hybrid propulsion, multi-objective trajectory optimization

1. Introduction

An electric solar wind sail (E-sail) consists of a number of charged tethers kept at a high positive voltage that interact with the solar wind ions to generate a propulsive acceleration [1]. In its originally-proposed configuration [2], an E-sail should be a large structure, with dimensions on the order of tens of kilometers and composed by hundreds to thousands tethers. However, due to the difficulty of deploying an controlling a huge tether structure in deep space, recent works suggest that near-term E-sail missions should involve small satellites with a limited number of spin-stabilized thrust-generating tethers [3]. Accordingly, the expected magnitude of the propulsive acceleration is small. Moreover, a recent E-sail thrust model suggests that the thrust vector is constrained within a cone with half-angle lesser than 20 degrees centered along the outwards radial direction [4], thus limiting the E-sail capability of generating a significant circumferential thrust component.

A possible strategy to overcome the aforementioned issues consists of combining with a small E-sail with one or more high specific impulse electric thrusters. This strategy resembles the hybrid sail concept, which can be traced back to 2002 [5], and consists of a combination of a solar sail and an electric thruster. Possible applications of hybrid sails have been deeply investigated since, considering different heliocentric [6, 7, 8] and geocentric [9, 10] scenarios and ultimately leading to the design of a solar power sail to propel JAXA's OKEANOS mission (eventually not financed) towards a Jupiter Trojan asteroid [11, 12].

Like the hybrid sail concept, the combination of an E-sail and an electric thruster could significantly increase their effectiveness. The compatibility of an E-sail tether grid and an electric thruster as a field emission electric propulsion (FEEP) has been previously assessed in literature for attitude control purposes [13]. In analogy with previous works, several very small FEEP thrusters could be located on the remote units placed at the tip of the spinning tethers. Alternatively, a larger thruster could be placed onboard the spacecraft body, where a limited interaction with the one or few spinning charged tethers is expected. Accordingly, in this analysis it is assumed that the interaction between the two propulsive systems does not cause any efficiency reduction.

This work focuses on deep-space heliocentric transfers performed by a small spacecraft equipped with

*Corresponding author, lorenzo.niccolai@unipi.it

an electric sail composed of a limited number of tethers and an electric thruster. The power available for the electric thruster is assumed to be provided by solar panels only, and, as such, to scale with the inverse square heliocentric distance. A recent and accurate model [4] is used to describe the E-sail thrust contribution as a function of the tether spin plane attitude and the Sun-spacecraft distance. Orbital transfers are analyzed within an optimal framework, in which a suitable performance index consisting in the combination of the flight time and the propellant consumption (with different relative weights) is minimized. It is assumed that the E-sail and the electric thruster can be steered independently. The solution of the optimal control problem makes use of an indirect multiple shooting method and is based on the Pontragyn's maximum principle [14]. Numerical simulations are performed in two circle-to-circle heliocentric transfer scenarios (Earth-Mars and Earth-Venus), and the transfer times are compared with those obtained with an E-sail alone, to quantify the advantage of the combination with an electric thruster.

2. Dynamical model

Consider a spacecraft equipped with a small E-sail and one (or more) electric thruster, powered by onboard solar panels. The spacecraft is performing a deep-space two-dimensional heliocentric transfer, so its dynamical equations can be conveniently written by using a heliocentric polar reference frame $\mathcal{T}(r,\theta)$, where r is the Sun-spacecraft distance and θ is a polar angle measured counterclockwise from a fixed direction. The latter is chosen so to coincide with the Sun-spacecraft direction at the initial time instant of the transfer $t_0 \triangleq 0$; see Fig. 1. The set of state variables of the system is completed by the radial velocity component u, the circumferential velocity component v, and the dimensionless spacecraft mass $m \triangleq M/M_0$, defined as the ratio of the instantaneous mass of the spacecraft M to the mass at the start of the transfer M_0. Accordingly, the dynamical equations of the spacecraft may be written as

$$\dot{r} = u \tag{1}$$

$$\dot{\theta} = \frac{v}{r} \tag{2}$$

$$\dot{u} = \frac{v^2}{r} - \frac{\mu_\odot}{r^2} + a_{ES_r} + a_{T_r} \tag{3}$$

$$\dot{v} = -\frac{uv}{r} + a_{ES_\theta} + a_{T_\theta} \tag{4}$$

$$\dot{m} = -\dot{m}_{\mathrm{ex}} \tag{5}$$

where $\mu_\odot$ is the Sun's gravitational parameter, and $\dot{m}_{\mathrm{ex}}$ is the dimensionless mass flow rate expelled by the electric

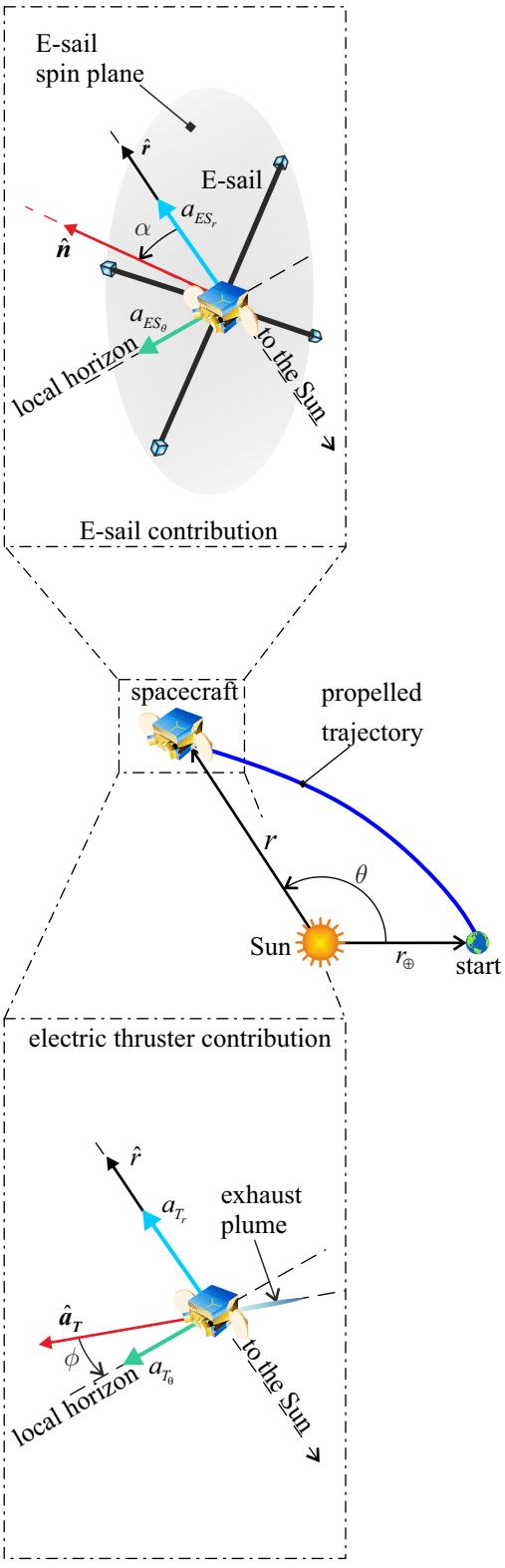

Figure 1: Sketch of the state variables and fundamental angles.

thruster. The a_{ES} and a_T terms in Eqs. (3) and (4) denote the propulsive acceleration provided by the E-sail and the electric thruster, respectively, and the subscripts r (or θ) identifies the radial (or circumferential) component. Therefore, a complete mathematical definition of the propulsive acceleration components provided by the E-sail and the electric thruster, as well as the expelled mass flow rate, is required to fully define the system dynamics.

2.1. E-sail propulsive acceleration model

The propulsive acceleration provided by the E-sail is generated by the electrostatic interaction between the ions immersed in the incoming solar wind and the charged tethers. Huo et al. [4] have analyzed the thrust generation assuming that the E-sail grid is axially-symmetric and kept stretched by the spacecraft spinning, and their results have been confirmed by more recent works [15]. The model presented in Ref. [4] is therefore consistent with a realistic near-term CubeSat spacecraft with a very limited number of spinning tethers. Accordingly, the propulsive acceleration generated by an E-sail is inversely proportional to the Sun-spacecraft distance and can be written as

$$\boldsymbol{a}_{ES} = \tau \frac{a_c}{2} \left(\frac{r_\oplus}{r} \right) [\hat{\boldsymbol{r}} + (\hat{\boldsymbol{r}} \cdot \hat{\boldsymbol{n}}) \hat{\boldsymbol{n}}] \tag{6}$$

where the characteristic acceleration a_c is an E-sail performance parameter corresponding to the maximum propulsive acceleration that the E-sail is able to generate at a reference Sun-spacecraft distance of $r_\oplus \triangleq 1$ au. Based on the results discussed in Refs. [16, 17, 18], the value of a_c is calculated as a function of the solar wind properties, namely, the plasma density at Sun-Earth distance $n_\oplus \simeq 3.6\,\mathrm{cm}^{-3}$, the solar wind velocity $v_{sw} \simeq 400\,\mathrm{km/s}$ and potential $V_{sw} \simeq 1\,\mathrm{kV}$, and the mass of the dominating ion species (i.e., the proton mass $M_p = 1.672 \times 10^{-27}$ kg), viz.

$$a_c = \frac{NLK\,(V_{ES} - V_{sw})\,\sqrt{\epsilon M_p n_\oplus v_{sw}^2}}{M_0} \left(\frac{1}{m} \right) \tag{7}$$

where an E-sail composed of N tethers, each one with length L and maintained at a (constant) potential V_{ES} is assumed. The parameter K in Eq. (7) is an empirical constant that, according to Refs. [16, 17], is set equal to 0.18, and $\epsilon \triangleq 8.854 \times 10^{-12}$ F/m is the vacuum permittivity. The instantaneous value of the characteristic acceleration given by Eq. (7) is affected by the mass variation due to propellant consumption, so Eq. (7) is rewritten so to express the instantaneous value of a_c as a function of the value calculated at the start of the transfer, yielding

$$a_c = a_{c_0} \left(\frac{1}{m} \right) \tag{8}$$

where a_{c_0} is obtained from Eq. (7) with $m = m(t_0) = 1$. Furthermore, in Eq. (6), $\tau \in [0, 1]$ represents a switching parameter that models the possibility of adjusting the power supplied to the electron gun required to maintain the tether voltage, $\hat{\boldsymbol{r}}$ is the outwards radial unit vector, and $\hat{\boldsymbol{n}}$ is the unit vector normal to the E-sail spinning plane in the direction opposite to the Sun. Note that Eq. (6) implies that both the magnitude and the direction of the E-sail-generated propulsive acceleration is strictly related to the E-sail attitude (i.e., the spin plane spatial orientation expressed by the unit vector $\hat{\boldsymbol{n}}$), similarly to what happens for a solar sail.

Based on Eq. (6), the propulsive acceleration components are obtained as

$$a_{ES_r} = \tau \frac{a_{c_0}}{2m} \left(\frac{r_\oplus}{r} \right) \left(1 + \cos^2 \alpha \right) \tag{9}$$

$$a_{ES_\theta} = \tau \frac{a_{c_0}}{2m} \left(\frac{r_\oplus}{r} \right) \cos \alpha \sin \alpha \tag{10}$$

where $\alpha \in [-\pi/2, \pi/2]$ is the angle between $\hat{\boldsymbol{r}}$ and $\hat{\boldsymbol{n}}$, measured counterclockwise; see Fig. 1. The E-sail acceleration components given by Eqs. (9) and (10) may be substituted into Eqs. (3) and (4) to model the E-sail effect on the spacecraft dynamics.

2.2. Electric thruster propulsive acceleration model

In this analysis, the spacecraft is assumed to be equipped with an electric engine providing a low thrust, such as a field emission electric propulsion (FEEP) or an ion thruster. Since a small spacecraft is considered in this work, the power cannot be provided by a radioisotope thermal generator (RTG), so the thruster must be fed by onboard solar panels. The amount of power received from the solar panels scale as the inverse square heliocentric distance, and it is assumed that the generated thrust is directly proportional to the amount of power fed to the thruster. Accordingly, and in analogy with Ref. [7], the propulsive acceleration provided by the electric thruster is written as

$$\boldsymbol{a}_T = \kappa \frac{a_{T_0}}{m} \left(\frac{r_0}{r} \right)^2 \hat{\boldsymbol{a}}_T \tag{11}$$

where $\kappa \in [0, 1]$ is a parameter that defines the amount of available power that is supplied to the thruster, the unit vector $\hat{\boldsymbol{a}}_T$ identifies the thrust direction, and the subscript 0 denotes the initial condition. In particular, a_{T_0} is the propulsive acceleration magnitude at the beginning

of the transfer, and can be seen as a thruster performance parameter.

In analogy with previous works, the direction of the thrust contribution generated by the electric engine is identified by defining the thrust angle $\phi \in [\phi_{min}, \phi_{\max}]$ as the angle between $\hat{\boldsymbol{a}}_T$ and the local horizon, measured counterclockwise; see Fig. 1. The admissible values of the thrust angle take into account limitations in the steering capability of the thruster and possible constraints on the direction of the exhaust ions expelled that should not impinge on the E-sail tethers. Based on the thrust angle definition, the electric thruster contribution to the spacecraft propulsive acceleration may be decomposed into a radial and a circumferential component as

$$a_{T_r} = \kappa \frac{a_{T_0}}{m} \left(\frac{r_0}{r}\right)^2 \sin\phi \tag{12}$$

$$a_{T_\theta} = \kappa \frac{a_{T_0}}{m} \left(\frac{r_0}{r}\right)^2 \cos\phi \tag{13}$$

which may be substituted into Eqs. (3) and (4).

Finally, a complete definition of the system dynamics requires a mathematical expression of the dimensionless mass flow rate expelled by the electric thruster, to be inserted in Eq. (5). Specifically, the dimensionless mass consumption per time unit depends on the power that is supplied to the thruster, yielding [6]

$$\dot{m}_{\text{ex}} = \kappa \frac{a_{T_0}}{g I_{sp}} \left(\frac{r_0}{r}\right)^2 \tag{14}$$

where $g \triangleq 9.80665\,\text{m/s}^2$ is the standard gravity at Earth's sea level, and I_{sp} is the thruster specific impulse.

3. Optimal control problem formulation

Having fully characterized the system dynamics by obtaining a mathematical model for the terms involved in Eqs. (1)–(5), an orbital transfer with a spacecraft propelled by an E-sail and an electric thruster can be analyzed within an optimal framework. To this end, consider a circle-to-circle, two-dimensional, deep-space transfer from the Earth to a target celestial body whose heliocentric orbital eccentricity is neglected in this work.

First, it is assumed that the control variables that may independently selected at every time instant are the E-sail attitude angle α, its switching factor τ, the electric engine thrust angle ϕ and its power feeding factor κ. Then, the cost function J to be maximized is defined as a linear combination of the final (dimensionless) spacecraft mass and the negative flight time, viz.

$$J = \gamma m_f - (1-\gamma)\frac{t_f}{T} \tag{15}$$

where the subscript f denotes the end of the transfer, and $T \triangleq 2\pi\sqrt{r_0^3/\mu_\odot}$ is used as a reference time to obtain a dimensionless cost function. The expression of the cost function given by Eq. (15) highlights that the optimality of a transfer trajectory is defined by a trade-off between competing requirements, namely, performing the maneuver in a short flight time and using a small amount of propellant. In this regard, the weight $\gamma \in [0, 1]$ represents a trade-off parameter that defines the relative importance of the propellant-related objective with respect to the flight time objective. In particular, selecting $\gamma = 0$ amounts to searching for the minimum-time transfer trajectory regardless of the propellant consumption, while a value $\gamma = 1$ only minimizes the propellant consumption without taking into account the time required by the transfer.

The optimal control problem is then formulated by adding to the set of state variables of the system $\{r, \theta, u, v, m\}$ a set of costate (adjoint) variables $\{\lambda_r, \lambda_\theta, \lambda_u, \lambda_v, \lambda_m\}$, each one associated with a physical state variable. Accordingly, the system Hamiltonian function may be defined as [14]

$$\mathcal{H} \triangleq \lambda_r \dot{r} + \lambda_\theta \dot{\theta} + \lambda_u \dot{u} + \lambda_v \dot{v} + \lambda_m \dot{m} \tag{16}$$

where the time derivatives of the state variables are given by Eqs. (1)–(5). The time histories of the costate variables are obtained from the Euler-Lagrange equations as

$$\dot{\lambda_r} = -\frac{\partial H}{\partial r} \tag{17}$$

$$\dot{\lambda_\theta} = -\frac{\partial H}{\partial \theta} = 0 \tag{18}$$

$$\dot{\lambda_u} = -\frac{\partial H}{\partial u} = \frac{\lambda_v v}{r} - \lambda_r \tag{19}$$

$$\dot{\lambda_v} = -\frac{\partial H}{\partial v} = \frac{-\lambda_\theta - 2\lambda_u v + \lambda_v u}{r} \tag{20}$$

$$\dot{\lambda_m} = -\frac{\partial H}{\partial m} \tag{21}$$

where the explicit expressions of Eq. (17) and (21) are omitted for the sake of conciseness. Note that Eq. (18) highlights that λ_θ is a constant of motion.

3.1. Optimal control laws

According to Pontragyn's maximum principle, the optimal trajectory is obtained when the control variables $\{\tau, \alpha, \kappa, \phi\}$ are selected so to maximize the Hamiltonian given by Eq. (16). The portion of the Hamiltonian that explicitly depends on the control variables $\mathcal{H}'$ can be split into two separate contributions, viz.

$$\mathcal{H}' = \mathcal{H}'_{ES} + \mathcal{H}'_T \tag{22}$$

where the E-sail contribution $\mathcal{H}'_{ES}$ is given by

$$\mathcal{H}'_{ES} \triangleq \tau \frac{a_{c_0}}{2m}\left(\frac{r_\oplus}{r}\right)\left[\lambda_u\left(1+\cos^2\alpha\right)+\lambda_v\cos\alpha\sin\alpha\right] \tag{23}$$

while the electric thruster contribution $\mathcal{H}'_T$ can be expressed as

$$\mathcal{H}'_T \triangleq \kappa \frac{a_{T_0}}{m}\left(\frac{r_0}{r}\right)^2\left(\lambda_u\sin\phi+\lambda_v\cos\phi-\lambda_m\frac{m}{gI_{sp}}\right) \tag{24}$$

Assuming that the control variables can be freely selected at every time instant of the motion, the maximization of $\mathcal{H}'$ can be performed by independently maximizing the single contributions $\mathcal{H}'_{ES}$ and $\mathcal{H}'_T$. Paralleling the discussion provided in Ref. [4], the optimal values of the switching parameter $\tau^\star$ and the E-sail cone angle $\alpha^\star$ that maximize $\mathcal{H}'_{ES}$ are obtained as

$$\alpha^\star = \frac{1}{2}\arctan\left(\frac{\lambda_v}{\lambda_u}\right) \tag{25}$$

$$\tau^\star = \frac{1}{2}+\frac{1}{2}\text{sign}\left(1+\frac{3\lambda_u}{\sqrt{\lambda_u^2+\lambda_v^2}}\right) \tag{26}$$

Conversely, the maximum value of the portion of the Hamiltonian that depends on the electric thruster control variables $\mathcal{H}'_T$ is obtained by taking into account the admissible values of ϕ as

$$\phi^\star = \begin{cases} \phi_{\min} & \text{if} \quad \phi_{opt} < \phi_{\min} \\ \phi_{opt} & \text{if} \quad \phi_{\min} \le \phi_{opt} \le \phi_{\max} \\ \phi_{\max} & \text{if} \quad \phi_{opt} > \phi_{\max} \end{cases} \tag{27}$$

where the value of $\phi_{opt} \in [0, 2\pi)$ is calculated from the following conditions

$$\sin\phi_{opt} = \frac{\lambda_u}{\sqrt{\lambda_u^2+\lambda_v^2}} \qquad \cos\phi_{opt} = \frac{\lambda_v}{\sqrt{\lambda_u^2+\lambda_v^2}} \tag{28}$$

Finally, the optimal value of the power feeding parameter $\kappa^\star$ is obtained with a simple bang-bang control law

$$\kappa^\star = \frac{1}{2}+\frac{1}{2}\text{sign}\left(\lambda_u\sin\phi^\star+\lambda_v\cos\phi^\star-\lambda_m\frac{m}{gI_{sp}}\right) \tag{29}$$

which highlights that the electric thruster is either switched off ($\kappa^\star = 0$) or powered with the maximum available power ($\kappa^\star = 1$).

3.2. Boundary conditions

The dynamical equations (1)–(5) and the Euler-Lagrange equations (17)–(21) define a two-point boundary value problem, which is completed by a set of boundary conditions related to the system state at the start and the final time instant of the transfer. Assume that the spacecraft exits the Earth's sphere of influence with negligible hyperbolic excess velocity at time $t_0 \triangleq 0$, so that $r_0 = r_\oplus$, and let r_f be the heliocentric orbit radius of the target celestial body. Accordingly, the boundary conditions at the start of the transfer are given by

$$\begin{aligned} &r(0) = r_\oplus \qquad \theta(0) = 0 \qquad u(0) = 0 \\ &v(0) = \sqrt{\frac{\mu_\odot}{r_\oplus}} \qquad\qquad m(0) = 1 \end{aligned} \tag{30}$$

while the boundary conditions at the end of the transfer are

$$r(t_f) = r_f \qquad u(t_f) = 0 \qquad v(t_f) = \sqrt{\frac{\mu_\odot}{r_f}} \tag{31}$$

The problem needs to be completed by enforcing the transversality conditions [14], yielding

$$\lambda_\theta(t_f) = 0 \qquad \lambda_m(t_f) = \gamma \qquad \mathcal{H}(t_f) = \frac{1-\gamma}{T} \tag{32}$$

Note that the first of transversality conditions (32), combined with Eq. (18), shows that $\lambda_\theta \equiv 0$ for all $t \in [0, t_f]$. Accordingly, solving the optimal control problem amounts to finding the initial values of the costate variables $\{\lambda_r(0), \lambda_u(0), \lambda_v(0), \lambda_m(0)\}$ and the transfer time t_f, so that the boundary conditions (30), (31) and the transversality conditions (32) are met. It is evident that a different optimal solution will be obtained for each value of γ, which in turn expresses a different relative weight of the two competing requirements of short flight time and small propellant consumption.

4. Case study

The effectiveness of the previously discussed control law is tested in two exemplary mission scenarios, consisting of circle-to-circle, ephemeris-free, interplanetary transfers towards Mars or Venus. The spacecraft is assumed to be have a launch total mass $M_0 = 20\,\text{kg}$. A complete list of the E-sail data used in the numerical simulations is given in Tab. 1. The selected values are based on the preliminary mission design provided in Ref. [3], and are compatible with a near-term deep-space mission. The mass of the E-sail described in Tab. 1 has been estimated based on existing mass-budget breakdown models [13], considering a Heytether structure [19] and excluding components that are required only if a large grid is assumed, as auxiliary tethers. Under these assumptions, the E-sail system mass includes

a total tether mass of about 0.23 kg, a reel mass ranging from 0.24 kg (if $N = 1$ and $L = 20$ km) to 0.24 kg (if $N = 4$ and $L = 5$ km), and an E-sail-related power generation system mass of about 2.8 kg. Accordingly, the mass associated with the E-sail system is estimated to be about 3.5 kg, a value that is compatible with the total launch mass estimation.

Table 1: Characteristics of the E-sail used in the numerical simulations.

Quantity	Value	Measurement unit
NL	20	km
V_{ES}	20	kV
a_{c_0}	0.307	mm/s^2

The parameters of the electric thruster are taken from IFM Micro FEEP Thruster design, which is currently undergoing space-qualification tests [20] and should be fit into two CubeSat units, and are reported in Tab. 2. The total dry mass of the thruster is about 2.6 kg including the power processing unit. Note that the parameters of Tab. 2 are also compatible with a configuration in which a set of smaller FEEP thruster is placed inside the remote unit at the tip of each tether, assuming $N \geq 2$. The thrust direction is assumed to be steerable within a cone with half-angle 30 deg centered along the circumferential direction. The angle ϕ is assumed to be acute (or obtuse) for orbital transfers towards external (or internal) regions of the Solar System, so that the electric thruster propulsive acceleration has a positive (or negative) circumferential component a_{T_θ}.

Table 2: Characteristics of the electric thruster used in the numerical simulations.

Quantity	Value	Measurement unit
Nominal thrust	1.0	mN
I_{sp}	2 150	s
a_{T_0}	0.05	mm/s^2
Thrust cone half-angle	30	deg

The results for an Earth-Mars scenario (r_f = 1.524 au) are given in Fig. 2, where the Pareto front of the multi-objective optimization is plotted. In particular, different flight times and propellant consumptions are shown for different values of the trade-off constant γ. It

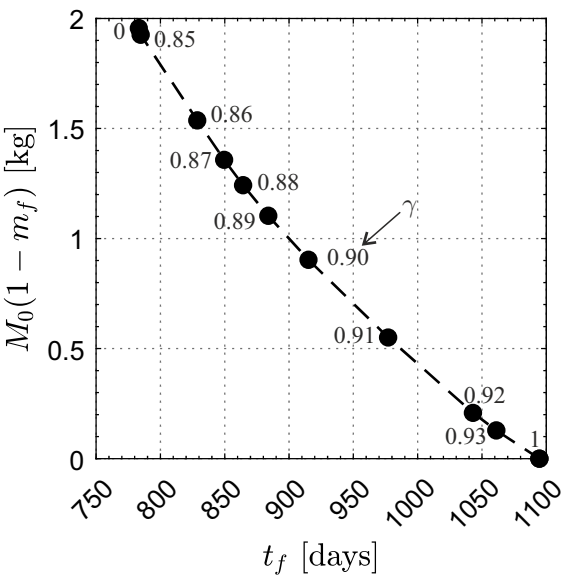

Figure 2: Pareto front of Earth-Mars transfer different values of γ.

is worth remarking that for $\gamma \in [0, 0.8]$, the optimal trajectories are almost identical, with the electric thruster firing for all of the flight time. Increasing the value of γ, the electric thruster is switched off for larger parts of the heliocentric transfer. When γ approaches 1, the solution of the optimal control problem tends to the limit case in which only the E-sail is used and the electric thruster is never switched on. The transfer time corresponding to the latter case is almost 3 years. Assuming a propellant consumption of about 1 kg [20] the flight time is reduced by 200 days, while the $\gamma = 0$ case (i.e., thruster always switched on and minimum-time trajectory) allows the flight time to be reduced by 320 days. The effectiveness of the combination of an E-sail and a high-specific impulse electric thruster is remarkable.

An example of optimal time histories of the control variables $\{\tau^\star(t), \alpha^\star(t), \kappa^\star(t), \phi^\star(t)\}$ calculated for an Earth-Mars transfer setting $\gamma = 0.86$ is given in Fig. 3. Note that the thruster is switched on for the majority of the flight time, consuming a total propellant mass of 1.54 kg but allowing Mars to be reached in 829 days. A different situation is shown in Fig. 4, where an optimal Earth-Mars transfer with $\gamma = 0.91$ is considered. In this scenario, the transfer is mostly E-sail-propelled, with the thruster switching on for short firing times. The transfer time is consequently larger with respect to the previous case, amounting to 977 days, but the propellant consumption is reduced to just 0.55 kg.

Considerations made for the Earth-Mars transfer can

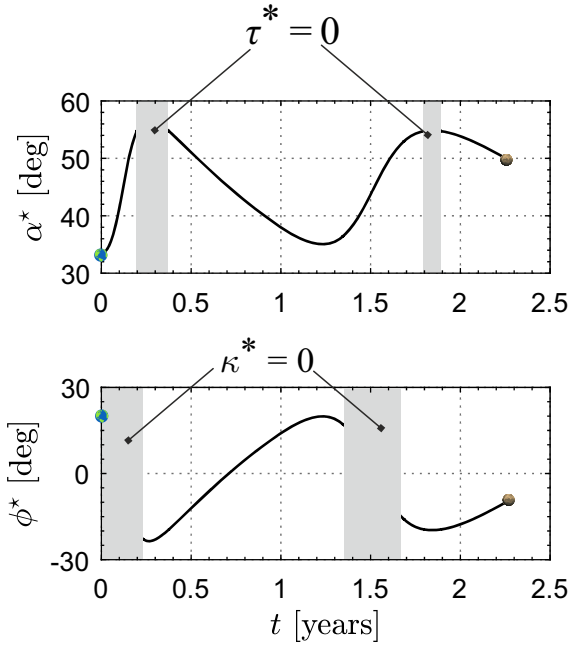

Figure 3: Time histories of the optimal control variables for an Earth-Mars transfer with $\gamma = 0.86$.

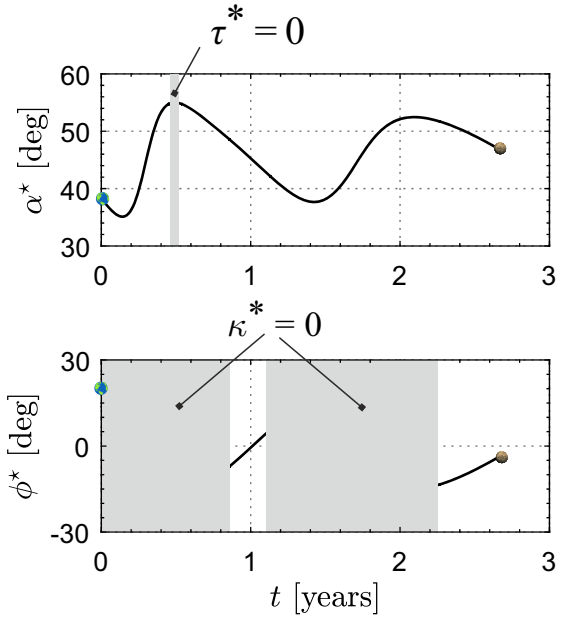

Figure 4: Time histories of the optimal control variables for an Earth-Mars transfer with $\gamma = 0.91$.

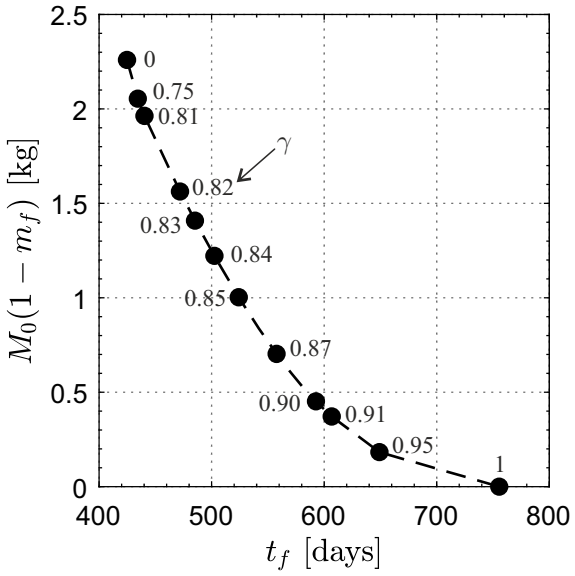

Figure 5: Pareto front of Earth-Venus transfer different values of γ.

be easily extended to an Earth-Venus transfer scenario. In this case, since $r_f = r_{\varphi} = 0.723$ au is lesser than $r(0) = r_{\oplus}$, the electric thruster is assumed to be placed onboard so to generate a negative circumferential thrust component a_{T_θ}, so $\phi \in [5\pi/6, 7\pi/6]$. The Pareto front generated by setting different values of γ is shown in Fig. 5. In this scenario, the global minimum of the transfer time amounts to 425 days (obtained with $\gamma = 0$) and the corresponding propellant consumption amounts to about 2.26 kg, while the transfer time if only the E-sail is used (i.e., $\gamma = 1$) is 756 days. A propellant consumption of 1 kg enables a significant flight time reduction, amounting to 232 days. These results suggest that the combination of an E-sail and an electric thruster proves its effectiveness even for orbital transfer towards inner regions of the solar system.

5. Conclusion

This work has discussed the possibility of combining an electric sail composed of a very small number of tethers with an electric thruster to perform deep-space heliocentric transfers. While the electric sail thrust scales as the inverse heliocentric distance, the power fed to the thruster has been assumed to scale as the power generated by onboard solar panels. The analysis has been performed within an optimal framework, in which a multi-objective cost function is minimized, consisting of the combination of the flight time and the propellant

consumption with different relative weights. Numerical simulations have shown the effectiveness of the combination of the sail and the thruster, with significant reduction of the transfer times obtained even with small propellant consumptions.

A natural extension of this work could assume that the electric sail is constantly kept in the Sun-facing configuration, thus significantly simplifying the attitude control. More refined developments could consist of the analysis of a scenario in which the sail attitude and the thruster exhaust direction cannot be freely selected but are coupled, and the extension to more realistic transfer trajectories (including planetary eccentricities and inclination with respect to the Ecliptic).

References

[1] M. Bassetto, L. Niccolai, A. A. Quarta, and G. Mengali. A comprehensive review of Electric Solar Wind Sail concept and its applications. *Progress In Aerospace Sciences*, 128(article no. 100768):1–27, 2022. doi: 10.1016/j.paerosci.2021.100768.

[2] P. Janhunen. Electric sail for spacecraft propulsion. *Journal of Propulsion and Power*, 20(4):763–764, 2004. doi: 10.2514/1.8580.

[3] A. Slavinskis, P. Janhunen, P. K. Toivanen, et al. Nanospacecraft fleet for multi-asteroid touring with electric solar wind sails. In *IEEE Aerospace Conference Proceedings*, volume 2018-March, pages 1–20, Big Sky (MT), USA, March 3–10 2018. doi: 10.1109/AERO.2018.8396670.

[4] M. Huo, G. Mengali, and A. A. Quarta. Electric sail thrust model from a geometrical perspective. *Journal of Guidance, Control, and Dynamics*, 41(3):734–740, 2018. doi: 10.2514/1.G003169.

[5] M. Leipold and M. Götz. Hybrid photonic/electric propulsion. techreport, Munich, Germany, 2002.

[6] G. Mengali and A. A. Quarta. Trajectory design with hybrid low-thrust propulsion system. *Journal of Guidance, Control, and Dynamics*, 30(2):419–426, 2007. doi: 10.2514/1.22433.

[7] G. Mengali and A. A. Quarta. Tradeoff performance of hybrid low-thrust propulsion system. *Journal of Spacecraft and Rockets*, 44(6):1263–1270, 2007. doi: 10.2514/1.30298.

[8] R. J. McKay, M. Macdonald, J. D. Biggs, and C. R. McInnes. Survey of highly-non-Keplerian orbits with low-thrust propulsion. *Journal of Guidance, Control, and Dynamics*, 34(3):645–666, May 2011. doi: 10.2514/1.52133.

[9] M. Ceriotti and C. R. McInnes. Generation of optimal trajectories for Earth hybrid pole sitters. *Journal of Guidance, Control, and Dynamics*, 34(3):847–859, May 2011. doi: 10.2514/1.50935.

[10] J. Heiligers, C. R. McInnes, J. D. Biggs, and M. Ceriotti. Displaced geostationary orbits using hybrid low-thrust propulsion. *Acta Astronautica*, 71:51–67, February 2012. doi: 10.1016/j.actaastro.2011.08.012.

[11] O. Mori, J. Matsumoto, T. Chujo, et al. Solar power sail mission of OKEANOS. *Astrodynamics*, 4(3):233–248, September 2020. doi: 10.1007/s42064-019-0067-8.

[12] M. Matsushita, T. Chujo, J. Matsumoto, et al. Solar power sail membrane prototype for OKEANOS mission. *Advances in Space Research*, 67(9):2899–2911, May 2021. doi: 10.1016/j.asr.2020.10.007.

[13] P. Janhunen, A. A. Quarta, and G. Mengali. Electric solar wind sail mass budget model. *Geoscientific Instrumentation, Methods, and Data Systems*, 2(1):85–95, February 2013. doi: 10.5194/gi-2-85-2013.

[14] A. E. Bryson and Y.-C. Ho. *Applied Optimal Control: Optimization, Estimation and Control*, chapter 2, pages 42–89. Hemisphere Publishing Corporation, New York (NY), USA, 1975.

[15] M. Bassetto, G. Mengali, and A. A. Quarta. Thrust and torque vector characteristics of axially-symmetric E-sail. *Acta Astronautica*, 146:134–143, May 2018. doi: 10.1016/j.actaastro.2018.02.035.

[16] P. Janhunen, P. K. Toivanen, J. Polkko, et al. Electric solar wind sail: toward test missions. *Review of Scientific Instruments*, 81 (11):1–111, November 2010. doi: 10.1063/1.3514548.

[17] P. K. Toivanen and P. Janhunen. Spin plane control and thrust vectoring of electric solar wind sail. *Journal of Propulsion and Power*, 29(1):178–185, January 2013. doi: 10.2514/1.B34330.

[18] P. K. Toivanen and P. Janhunen. Thrust vectoring of an electric solar wind sail with a realistic shape. *Acta Astronautica*, 131: 145–151, February 2017. doi: 10.1016/j.actaastro.2016.11.027.

[19] T. Rauhala, H. Seppänen, J. Ukkonen, et al. Automatic 4-wire Heytether production for the electric solar wind sail. In *The International Microelectronics Assembly and Packing Society Topical Workshop and Tabletop Exhibition on Wire Bonding*, San Jose (CA), USA, 2013.

[20] L. Grimaud, D. Krejci, and B. Seifert. The IFM Micro FEEP thruster: a modular design for smallsat propulsion. In *36th International Electric Propulsion Conference*, Vienna, Austria, September 2019.